

The change in boundary values due to moderate gain should produce small inaccuracies, of the order of a few percent, if the low-gain model is used to describe giant-pulse laser energy release.

Of the assumptions used in proving minor differences between the two cases, the assumption of uniform

photon density and distribution of the effect of standing waves is the greatest source of potential inaccuracy. This is because higher gain values reduce the influence of the standing wave and the spatially varying part of inversion and thereby change the value of  $\bar{N}$  rather than altering Eq. (B26) because of moderate values of  $\bar{N}$ .

## Optical Properties of Thin Germanium Films in the Wavelength Range 2000–6000 Å\*

PAUL M. GRANT† AND WILLIAM PAUL

*Division of Engineering and Applied Physics, Harvard University, Cambridge, Massachusetts*

(Received 3 February 1966; in final form 1 April 1966)

Measurements have been made of the normal incidence reflectivity and transmissivity coefficients  $R$  and  $T$  of thin germanium films. Films were deposited *in vacuo* on fused quartz substrates where the crystalline perfection of the film was controlled by varying the substrate temperature so that the effect of crystalline order on reflectivity could be observed. Epitaxial films were grown on cleaved  $\text{CaF}_2$  substrates to thicknesses in the range 100–3000 Å. Structure in the reflectivity and transmission spectra showed these films to possess bulk band properties. However, the amplitudes of  $R$  and  $T$  were affected by the presence of film surface roughness believed to originate from nucleation and growth phenomena. Also, compressive strain induced by the difference in thermal expansion coefficients between Ge and  $\text{CaF}_2$  shifted interband transition structure to slightly higher energies. Values of the optical constants were deduced from  $R$  and  $T$ . When experimental and calculational difficulties peculiar to the film method are accounted for, the results correspond closely to those of the Kramers–Kronig analyses of bulk reflectivity data.

### I. INTRODUCTION

IN this paper we examine the degree to which optical properties derived from measurements of semiconductors in the form of films can be correlated with optical properties of the materials in the bulk state. The problem chosen for detailed study was the determination of the optical properties of germanium films from reflection and transmission measurements. Much is known concerning the band structure of bulk crystalline germanium, which, in addition to the fact that films of this material are easily prepared in a variety of stages of crystalline perfection, makes it ideally suited for this investigation. This section summarizes the results of reflectivity measurements on bulk crystals and also previous film work. Section II contains a discussion of the film preparation techniques and optical apparatus used in this work. Section III presents results for the reflectivity and transmissivity coefficients of polycrystalline and epitaxial films. Section IV includes the calculation of the optical constants from the data of Sec. III, and Sec. V contains a discussion of the over-all results and conclusions.

\* This research was supported by the U. S. Office of Naval Research and formed part of a thesis submitted by P. M. Grant to the Division of Engineering and Applied Physics, Harvard University, in partial fulfillment of the requirements for the Ph.D. degree.

† IBM Pre-doctoral Fellow. Present address: IBM Research Laboratory, San Jose, California.

Energy band calculations<sup>1–3</sup> in conjunction with reflectivity experiments<sup>4–8</sup> have led to an understanding of the nature of interband transitions at energies up to 20 eV greater than the forbidden gap. The pseudopotential energy bands of germanium have been calculated by Brust<sup>2</sup> and are shown in Fig. 1 along with the important critical point transitions.  $M_0$ ,  $M_1$ , and  $M_2$  designate the type of critical point behavior and are explained in Ref. 2. Figure 2 depicts the reflectivity of bulk single-crystal germanium in the region of 2000 to 6000 Å as found by several workers.<sup>4,7,8</sup> The  $(L_3' \rightarrow L_1)$  and  $(\Lambda_3 \rightarrow \Lambda_1)$  transitions are responsible for the reflectivity peaks near 6000 Å; the  $L$  transition is thought to cause the onset of these peaks, while the peaks themselves are due to the  $\Lambda$  transition. Two peaks occur in the spectrum because of the spin-orbit splitting (not shown in Fig. 1) of the  $\Lambda_3$  valence band. The main peak near 2800 Å is due to the combined effect of the  $(X_4 \rightarrow X_1)$

<sup>1</sup> J. C. Phillips and L. Kleinman, *Phys. Rev.* **116**, 287 (1959).

<sup>2</sup> D. Brust, *Phys. Rev.* **134**, A1337 (1964).

<sup>3</sup> D. Brust, J. C. Phillips, and F. Bassani, *Phys. Rev. Letters* **9**, 94 (1962).

<sup>4</sup> H. R. Philipp and E. A. Taft, *Phys. Rev.* **113**, 1002 (1959).

<sup>5</sup> J. Tauc and E. Antoncik, *Phys. Rev. Letters* **5**, 253 (1960).

<sup>6</sup> H. Philipp and H. Ehrenreich, *Phys. Rev.* **129**, 1550 (1963).

<sup>7</sup> J. Tauc and A. Abraham, *Proceedings of the International Conference on Semiconductor Physics, Prague, 1960* (Czechoslovakian Academy of Sciences, Prague, 1961), p. 375; *J. Phys. Chem. Solids* **20**, 190 (1961).

<sup>8</sup> T. M. Donovan, E. J. Ashley, and H. E. Bennett, *J. Opt. Soc. Am.* **53**, 1403 (1963).

and ( $\Sigma_4 \rightarrow \Sigma_1$ ) transitions,<sup>2</sup> and the small peak near 2100 Å has been assigned to the ( $L_3' \rightarrow L_3$ ) transition which is not explicitly designated in Fig. 1. As Fig. 2 shows, agreement exists among the various workers as regards structure in the reflectivity spectrum; however, there are differences in the absolute amplitudes due to differences in sample surface preparation. Donovan *et al.*<sup>8</sup> have obtained the best reflectivity values yet by using electropolished surfaces, and their results are used as the standard in this paper. By using dispersion theory (Kramers-Kronig analysis), the optical constants have been deduced from the reflectivity data of Philipp and Taft<sup>4</sup> and more recently by Philipp<sup>9</sup> from that of Ref. 8. The results are given in Fig. 3 and will be compared to those obtained from film data. Figure 4 gives the skin depth  $\delta$  ( $\delta \equiv 1/\alpha \equiv \lambda/4\pi k$ ) for germanium from which one can see that very thin samples are necessary to perform transmission measurements in the range of 2–6 eV.

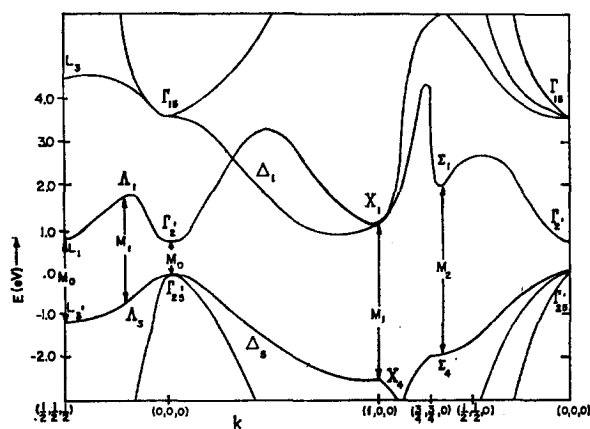


FIG. 1. The pseudopotential energy bands of germanium as calculated by Brust with some of the principal transitions indicated.

Previous measurements<sup>10–13</sup> of the optical properties of thin germanium films showed little resemblance to those of bulk material. Gebbie<sup>12</sup> appears to have been first to appreciate the importance of crystalline perfection and its effect on optical properties. He found that annealing his films after deposition for several hours at temperatures up to 525°C produced an electron diffraction pattern of fine Debye-Scherrer-Hull rings characteristic of the polycrystalline state. The optical constants for such a film are shown in Fig. 5 along with those of Ref. 9. Here the qualitative agreement among the values of  $k$  is tolerable, but  $n$  appears to oscillate wildly. Since this work is unpublished, we cannot be sure of the method used to obtain  $n$  and  $k$ . However, it

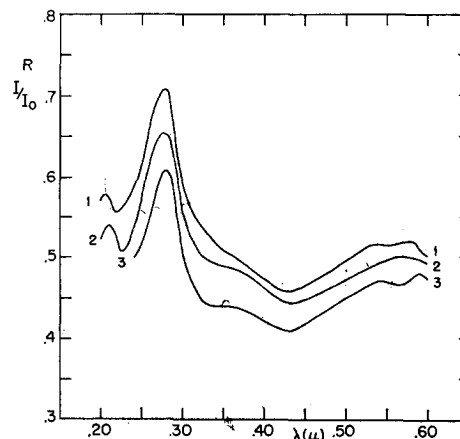


FIG. 2. Reflectivity of bulk germanium. 1. Donovan *et al.* (Ref. 8); 2. Philipp and Taft (Ref. 4); 3. Tauc and Abraham (Ref. 7).

is reported by Heavens<sup>14</sup> that Gebbie employed the transmittances of two or more films to deduce the optical constants. If this is the case, then the theory of Ref. 15 provides an explanation for the oscillatory behavior of  $n$  which shows it to be an effect of the method of calculation and not an intrinsic property of the material.

The most recent optical constant results are those of Lukeš,<sup>13</sup> shown in Fig. 6. These display fair qualitative agreement with the dispersion results over a common

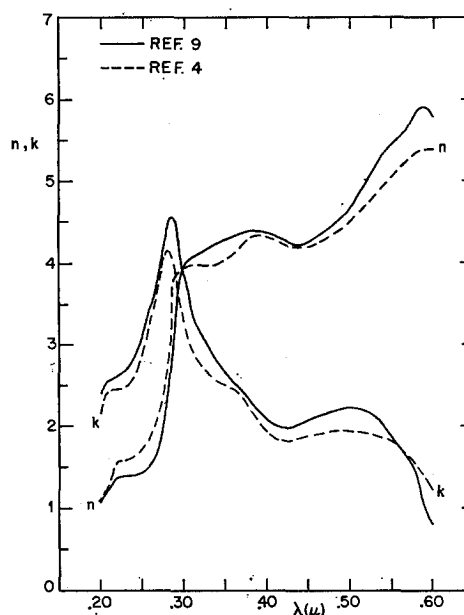


FIG. 3. The optical constants of germanium as obtained by Kramers-Kronig analyses.

<sup>9</sup> H. R. Philipp (private communication).

<sup>10</sup> H. M. O'Bryan, *J. Opt. Soc. Am.* **26**, 122 (1936).

<sup>11</sup> W. H. Brattain and H. B. Briggs, *Phys. Rev.* **75**, 1705 (1949).

<sup>12</sup> H. A. Gebbie, Ph.D. thesis, Reading, 1952 (unpublished), according to Ref. 13.

<sup>13</sup> F. Lukeš, *Czech. J. Phys.* **B10**, 59 (1960).

<sup>14</sup> O. S. Heavens, *Optical Properties of Thin Solid Films* (Butterworths Scientific Publications Ltd, London, 1953).

<sup>15</sup> P. M. Grant, *J. Opt. Soc. Am.* (to be published); P. M. Grant, *Bull. Am. Phys. Soc.* **10**, 546 (1965); P. M. Grant, Gordon McKay Laboratory of Applied Science, Harvard University, Technical Report No. HP-14, 1965 (unpublished), CFSTI AD-619071.

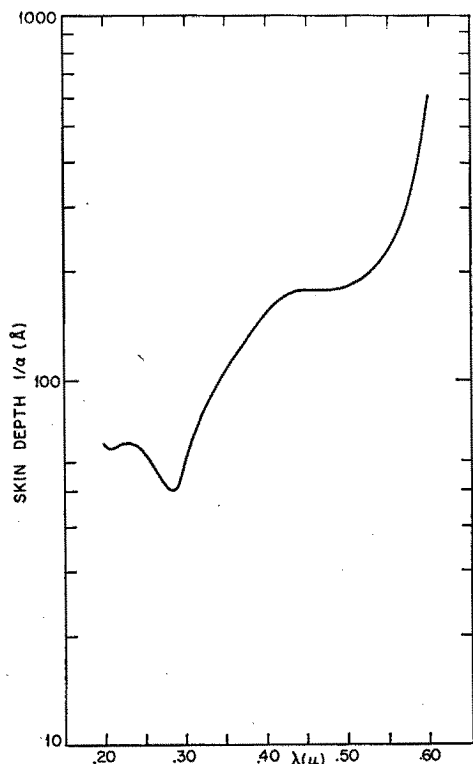


FIG. 4. Skin depth of germanium as a function of wavelength.

wavelength region. This is somewhat surprising because his films were neither deposited on hot substrates nor post-annealed to improve their crystallinity. That the crystallinity was indeed poor can be seen from his Fig. 5 which shows the reflectivity of one of his films. It cor-

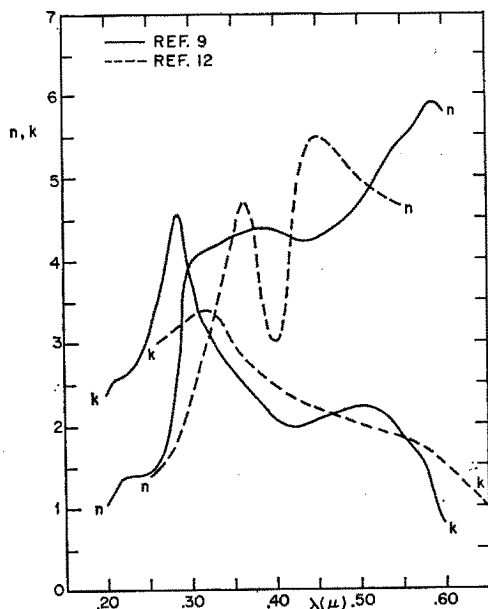


FIG. 5. Optical constants obtained by Gebbie from germanium thin films, shown by the broken line. The solid line indicates Philipp's calculations from the data of Donovan *et al.*

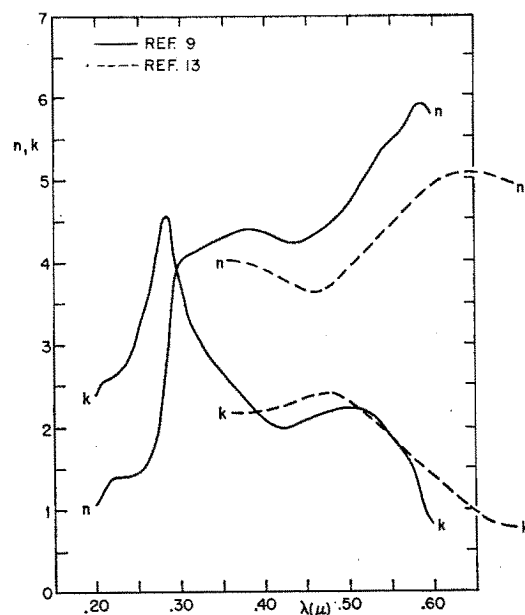


FIG. 6. Optical constants obtained by Lukeš from germanium thin films, shown by the broken line. The solid line indicates Philipp's calculations from the data of Donovan *et al.*

responds roughly to our result for a film on fused quartz shown by curve 4 of Fig. 9 which was definitely known to be of poor crystalline quality.

Measurements of either the transmissivity or reflectivity (but not both) of thin germanium films have been reported by Donovan and Ashley,<sup>16</sup> Tauc *et al.*,<sup>17</sup> and Cardona and Harbeke.<sup>18</sup> In the case of Refs. 16 and 17, only the reflectivity was measured and the relationship of their work to ours is studied in Sec. III. Cardona and Harbeke have measured the transmissivity (but not reflectivity) of several rather thick epitaxial films on  $\text{CaF}_2$ . Their total results account for the proper interband transitional structure; however, the magnitude of their transmissivities is in great disagreement with those calculated from bulk optical constants for the stated thicknesses.

## II. EXPERIMENTAL PROCEDURES

### A. Film Preparation

Vacuum deposition techniques were used to prepare film samples on both fused quartz and  $\text{CaF}_2$  substrates. The vacuum system was comprised of a 4-in. oil diffusion pump together with a mechanical forepump and liquid-nitrogen cold trap. Using the cold trap, this system was capable of maintaining pressures of  $1\text{--}3 \times 10^{-6}$

<sup>16</sup> T. M. Donovan and E. J. Ashley, *J. Opt. Soc. Am.* **54**, 1141 (1964).

<sup>17</sup> J. Tauc, A. Abraham, L. Pajasova, R. Grigorovici, and A. Vancu, in *Proceedings of the International Conference on Physics of Non-Crystalline Solids, Delft, 1964*, J. A. Prins, Ed. (Interscience Publishers, New York, 1965).

<sup>18</sup> M. Cardona and G. Harbeke, *J. Appl. Phys.* **34**, 813 (1963).

Torr during evaporation. The germanium source material was heated to evaporation temperatures in a tungsten boat of 0.005-in. thickness. The substrates were held about 6 in. above the source and were clipped to a 0.020-in. Ta plate with 0.005-in. Ta spring clips. This assembly was then heated from above by a series of 0.015-in.-diam Ta wire heater coils. The substrate temperature was measured by a Pt-Pt 10% Rh thermocouple held on the substrate surface with one of the Ta clips. The general procedure was to outgas the source and bake out the substrate for about 5 min before releasing a shutter and exposing the substrate to the evaporant beam.

A survey was made of possible substrate materials suitable for heteroepitaxial deposition of germanium. The following factors were taken into consideration:

(a) The substrate must be transparent to radiation with wavelength between 2000 and 6000 Å so that optical transmission measurements could be made on the deposited film.

(b) The present data on heteroepitaxy appear to suggest that the film and substrate lattice structure and lattice constants must match each other to a degree depending on the extent to which the bonding of the film material is ionic. That is, it seems that the greater the ionicity of the valence bonds of the film, the greater is the lattice mismatch with the substrate that can be tolerated. Therefore, as the germanium bond is non-ionic in character, a reasonable match of its lattice constant to that of the substrate is to be demanded.

(c) Because the substrate must be heated, it has to be able to withstand the temperature necessary for epitaxial growth without undue deterioration. Since this temperature runs between 500° and 700°C, the melting point of the substrate should be considerably above this range.

(d) Again, because the substrate must be heated, its linear thermal expansion coefficient becomes an important parameter. If the difference between the film and substrate thermal expansion coefficients is large, then large stresses are induced into the film on cooling to room temperature. This effect is discussed in Sec. III.

Of the presently available optical crystals,  $\text{CaF}_2$  and  $\text{SrF}_2$  come closest to satisfying all of the above criteria. We chose  $\text{CaF}_2$  for our work primarily because of the abundance of experience with this material as a substrate for germanium films.<sup>19-22</sup> The substrates were prepared by cleavage in air from a large single crystal. The resulting slab was 1 cm square by 1-2 mm thick. Sometimes several attempts were required to obtain a fairly smooth substrate surface. That is, the substrates, although being smooth on an atomic scale, would usually display a proliferation of cleavage steps on a macro-

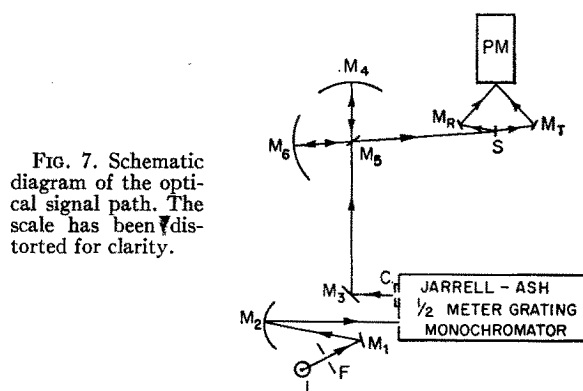


FIG. 7. Schematic diagram of the optical signal path. The scale has been distorted for clarity.

scopic level. The substrates were usually used immediately, but at other times several days would elapse. This did not seem to make any difference in the growth of the film. The fused quartz substrates were the same size as those of  $\text{CaF}_2$  and were prepared for deposition by washing in  $\text{HNO}_3$  and acetone.

The crystal structure of the deposited film was investigated using reflection electron diffraction and its surface topography studied by optical microscopy. The latter revealed the presence of surface roughness in those films deposited at high substrate temperatures and low deposition rates. Such behavior has been observed by several workers<sup>17,23,24</sup> and leads to degradation of the film optical response. This is further discussed in Sec. III.

Of the various methods available for film thickness measurement we chose infrared transmissivity. In the wavelength region above 1.8  $\mu$ , germanium may be treated as a dielectric. In this spectral range, the index of refraction appears to be rather independent of crystalline order so the method was applied to all films, whether epitaxial or polycrystalline. The rms deviation for measurements made on any one film was about 20 Å.

## B. Optical Measurements

Figure 7 is a schematic diagram of the optical path of the spectrophotometric system used to make measurements of the optical response coefficients. Light from the lamp L passes through filter F and is focused by the mirror system  $M_1$ ,  $M_2$  onto the entrance slit of a  $\frac{1}{2}$ -m Ebert grating monochromator manufactured by Jarrell-Ash Company. Monochromatic light emerges and passes through chopper C and is then focused by the "mirror lens" system  $M_4$ ,  $M_5$ ,  $M_6$  onto the sample S. It is easily seen that if the mirrors  $M_R$  and  $M_T$  are identical and the optical paths  $S \rightarrow M_T \rightarrow \text{PM}$  and  $S \rightarrow M_R \rightarrow \text{PM}$  are equal, then both transmissivity and reflectivity can be measured by a simple sample-in-sample-out technique. The mirrors were aluminized together and care was taken in alignment to keep the

<sup>19</sup> J. Marucchi and N. Nifontoff, *Compt. Rend.* **249**, 435 (1959).

<sup>20</sup> G. G. Via and R. E. Thun, *Natl. Symp. Vac. Technol. Trans.* **8**, 950 (1962).

<sup>21</sup> B. W. Sloope and C. O. Tiller, *J. Appl. Phys.* **33**, 3458 (1962).

<sup>22</sup> A. Catlin, A. J. Bellemore, Jr., and R. R. Humphris, *J. Appl. Phys.* **35**, 251 (1964).

<sup>23</sup> B. W. Sloope and C. O. Tiller, *Japan. J. Appl. Phys.* **2**, 308 (1963).

<sup>24</sup> R. S. Sennett and G. D. Scott, *J. Opt. Soc. Am.* **40**, 203 (1950).

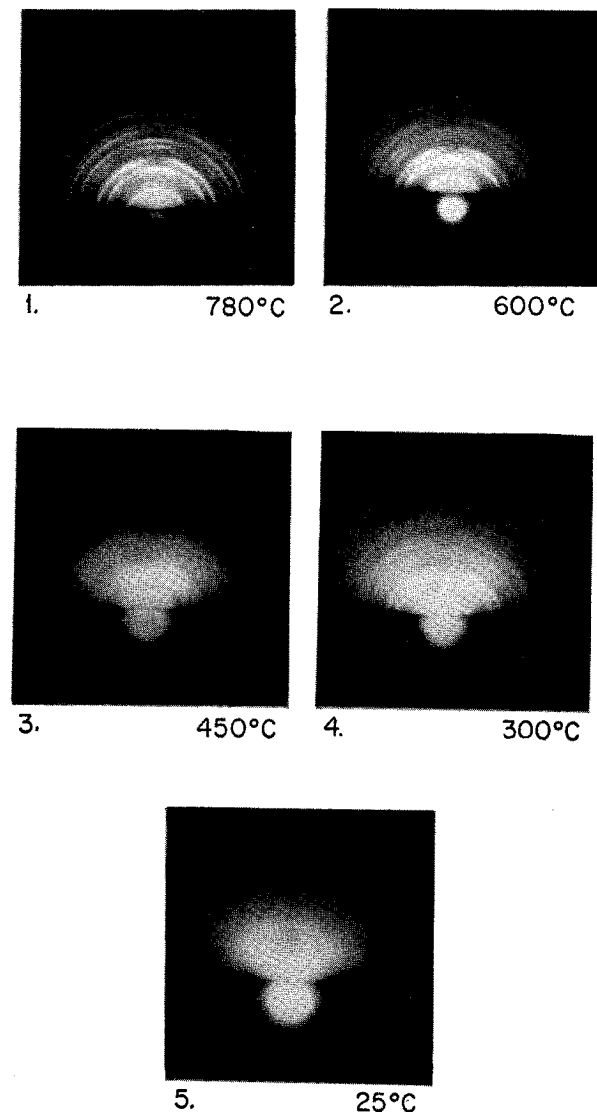


FIG. 8. Reflection electron diffraction patterns of Ge films deposited on fused quartz at various substrate temperatures. The deposition rate was from 120 to 220 Å/min for all films except film 1, where the high substrate temperature made it necessary to raise the deposition rate to 3000 Å/min in order to form a film.

optical path lengths as equal as possible. The average angle of incidence was  $7^\circ$ , essentially normal incidence. A tungsten lamp was used as the light source for the range 6000–3500 Å, while a high-pressure deuterium discharge device provided source energy down to 2000 Å. The photomultiplier detector was an EMI 6256B and the technique of phase sensitive detection was used in the electronic portion of the system.

The most difficult part of the experimental procedure was aligning the optics for the measurement of absolute reflectivity. Use of cleaved substrates made necessary a search for large film areas sufficiently level to allow optical alignment over the whole wavelength region. By carefully scanning the sample surface, we were us-

ually able to find an area flat enough to accommodate the slit image (about  $2\text{ mm} \times 0.5\text{ mm}$ ). In order to assure that absolute reflectivity was being measured, a bulk germanium sample was prepared by careful polishing and etching and its reflectivity taken in order to compare with values found by other workers. With a freshly etched surface, repetition of the alignment and measurement procedure indicated a scatter in the over-all reflectivity amplitude of  $\pm 0\%$ ,  $-2\%$  absolute in the wavelength region 3500–6000 Å and  $\pm 1\%$ ,  $-4\%$  absolute in the wavelength region 2000–3500 Å about the values of Ref. 8. For our purposes, this degree of accuracy was considered sufficient.

Alignment errors in the measurement of film transmissivity are thought to be small. Care was taken to keep observations in a pinhole-free region; however, some error was probably caused by substrate refraction. Errors of this type are estimated to be about 10% relative. On the other hand, scattered light considerations limited the transmission measurements to values above  $10^{-3}$ .

### III. RESULTS FOR THE FILM REFLECTIVITY AND TRANSMISSIVITY COEFFICIENTS

#### A. Polycrystalline Films

Figure 8 displays the reflection electron diffraction (RED) patterns for five germanium films deposited on fused quartz substrates held at different substrate temperatures. We see from the broadening of the Debye-Scherrer-Hull rings that there is a progressive decrease in grain size with decreasing substrate temperature. The effect on the film reflectivity can be seen in Fig. 9. Interference effects due to low absorption and film thinness appear at wavelengths above 3500 Å; hence care

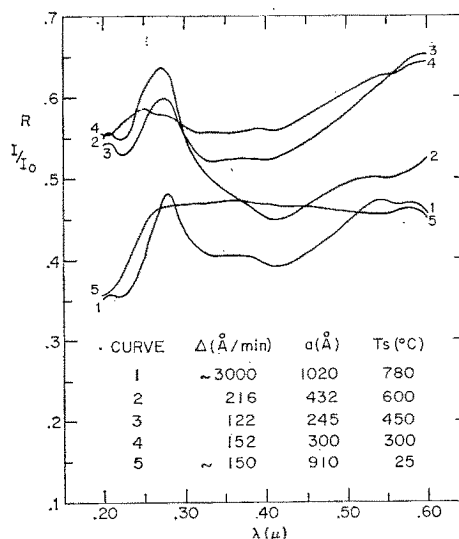


FIG. 9. Reflectivity of Ge films on fused quartz for various substrate temperatures.  $\Delta$ =deposition rate,  $a$ =film thickness,  $T_s$ =substrate temperature.

must be exercised in interpreting effects in this region as intrinsic. However, below 3500 Å the absorption is sufficiently high so that the reflectivity is independent of thickness. In this range, we see that the shape of the  $\Sigma$ ,  $X$  peak deteriorates with decreasing grain size (or with DSH ring broadening) until it completely disappears in the film deposited at room temperature. It might be expected that polycrystalline germanium would have the same optical response as single-crystal germanium and this is true up to a point. However, it is clear that ultimately the crystallite size can become so small or internal strain so great that even short-range order is deeply perturbed. Tauc *et al.*<sup>17</sup> interpret the resulting reflectivity spectrum as that which would occur for interband transitions with only energy conserved. That is, strong singularities in the joint density of states no longer appear due to the breakdown of symmetry and all interband transitions can be considered as indirect. This interpretation accounts for the loss of sharp reflectivity structure as one proceeds to the amorphous state. One notices that the amplitude of the  $\Sigma$ ,  $X$  peak of film 1 is considerably below those of the other polycrystalline films. This is due to scattering of the incident uv light by a rough film surface arising from deposition at elevated substrate temperatures. The onset of roughness with increasing substrate temperatures is a well-known effect.<sup>17,24</sup> Trying to optimize the amplitude of the  $\Sigma$ ,  $X$  peak involves finding a temperature at which long-range order will still be present, yet surface roughness will not. Our best sample in this respect was the 600°C film 2 of Fig. 9 which gave a value of 64%, agreeing well with that of Ref. 16. The remaining difference with the bulk is probably due to a residual roughness effect.

The 780°C film 1 was thick enough to suppress most of the interference effects in the long-wavelength region. It is seen that this film possesses all of the bulk reflectivity structure except that the  $\Lambda$  spin-orbit split peaks are severely distorted. From a similar study of these peaks under different states of disorder, Donovan and Ashley<sup>16</sup> imply that, for bulk crystals, a reassignment from the spin-orbit splitting scheme to one in which the low-energy peak belongs to  $L$ -point transitions and the high-energy peak to  $\Lambda$ -point transitions should be considered. In fact, such could be the case for polished bulk surfaces or highly polycrystalline films; however, the former interpretation still seems to be the correct one for the bulk single crystals because:

(a) It accounts in a clear manner for the theoretically predicted spin-orbit splitting.

(b)  $\Lambda$  transitions occur at  $M_1$ -type saddle points while  $L$  transitions occur at  $M_0$ -type saddle points.<sup>3</sup> The former have the proper shape to produce reflectivity peaks whereas the latter would tend to produce at best weak ones.

(c) Pressure measurements of Zallen *et al.*<sup>25</sup> show that both peaks have the same pressure coefficient, as would be expected if they arose at the same point in  $k$  space.

(d) The  $L$  transitions have actually been observed apart from the  $\Lambda$  transitions by Greenaway<sup>26</sup> for GaAs and by Cardona and Greenaway<sup>27</sup> for ZnTe and CdTe.

Reflectivity measurements on polycrystalline Ge films evaporated on fused quartz substrates held at 600°C with deposition rates ranging from 154–3850 Å/min have been taken. The results indicated that variations of this parameter within the above range produced changes in the reflectivity spectrum and RED patterns that were much smaller than those caused by changes in substrate temperature and whose interpretation would be very difficult.

### B. Epitaxial Films on CaF<sub>2</sub>

The optical properties of over 40 epitaxial films on CaF<sub>2</sub> were examined. Figures 10–15 show the results for three typical films deposited under conditions felt to give good crystalline quality yet minimize surface roughness. Figure 10 gives the RED patterns for these films and clearly shows their epitaxial behavior. The

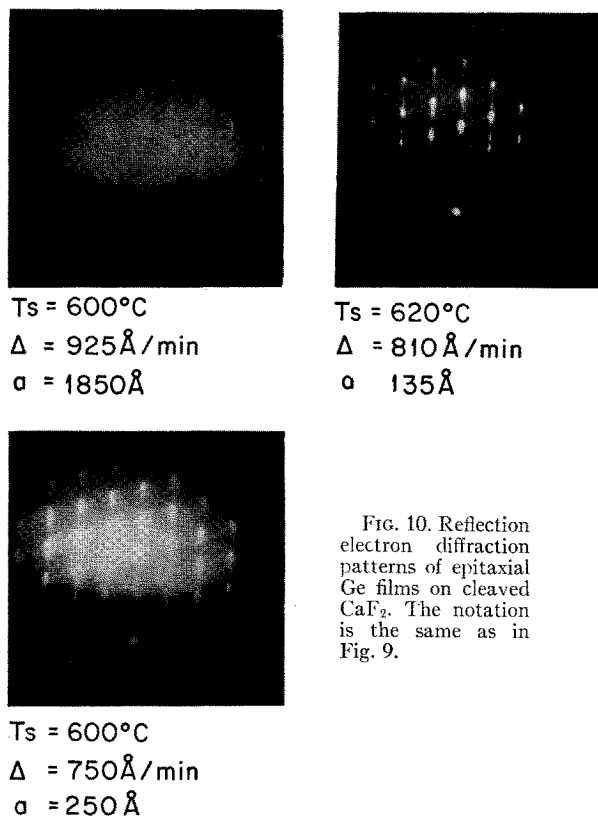


FIG. 10. Reflection electron diffraction patterns of epitaxial Ge films on cleaved CaF<sub>2</sub>. The notation is the same as in Fig. 9.

<sup>25</sup> R. Zallen, W. Paul, and J. Tauc, *Bull. Am. Phys. Soc.* **7**, 185 (1962); R. Zallen, Technical Report No. HP-12, Gordon McKay Laboratory of Applied Science, Harvard University, 1964 (unpublished).

<sup>26</sup> D. Greenaway, *Phys. Rev. Letters* **9**, 97 (1962).

<sup>27</sup> M. Cardona and D. Greenaway, *Phys. Rev.* **131**, 98 (1963).

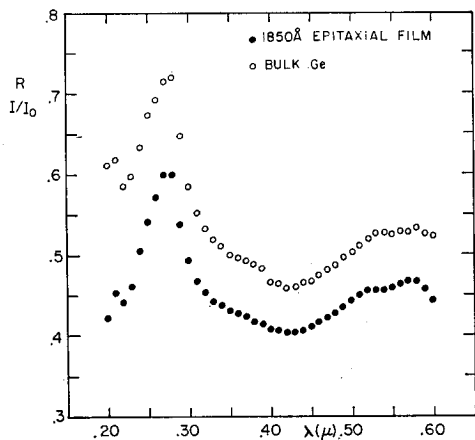


FIG. 11. Reflectivity of a 1850-Å epitaxial germanium film on  $\text{CaF}_2$  compared to that of bulk germanium.

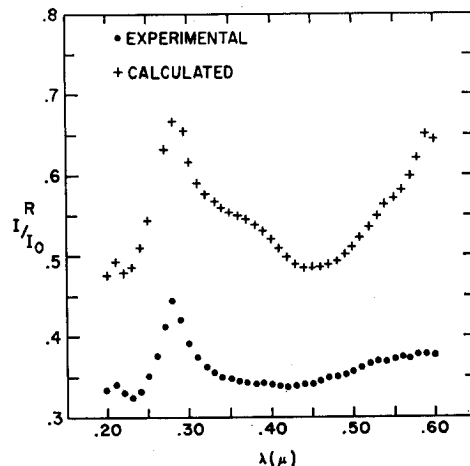


FIG. 14. Reflectivity of a 135-Å epitaxial film on  $\text{CaF}_2$  compared to theoretical values calculated from the data of Ref. 9.

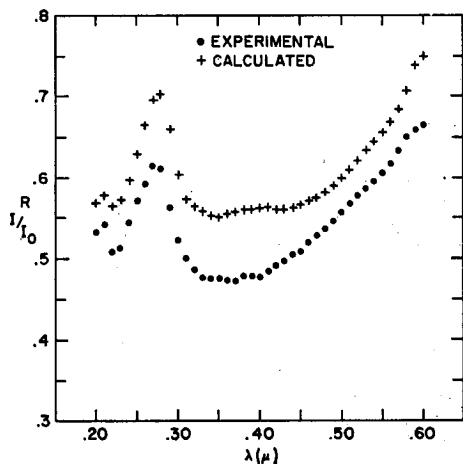


FIG. 12. Reflectivity of a 250-Å epitaxial film on  $\text{CaF}_2$  compared to theoretical values calculated from the data of Ref. 9.

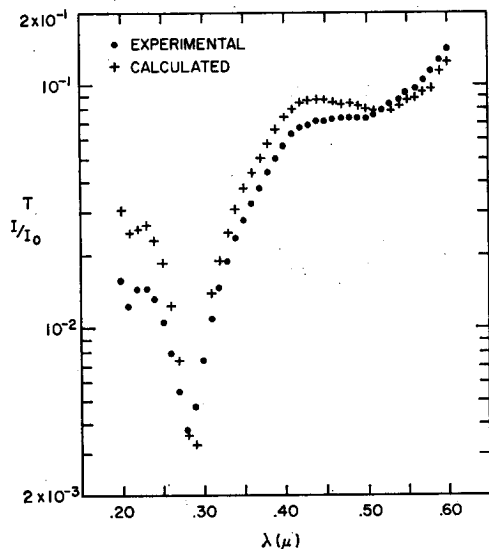


FIG. 13. Transmissivity of the same 250-Å film as in Fig. 12 compared to theoretical values calculated from the data of Ref. 9.

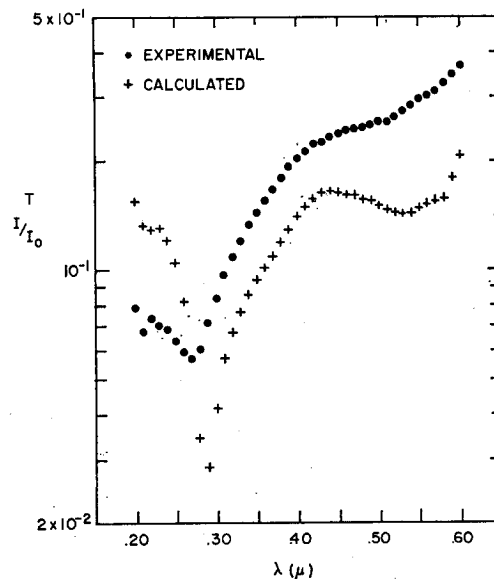


FIG. 15. Transmissivity of the same 135-Å film as in Fig. 14 compared to theoretical values calculated from the data of Ref. 9.

films are grown in the  $\langle 111 \rangle$  direction and the electron beam is incident in a  $\langle 110 \rangle$ -type direction. For epitaxial films, one would expect structure in the optical response to duplicate closely that of bulk material. Examination of Figs. 11–15 shows this to be true. Each epitaxial film has all the principal structure indicated by bulk reflectivity, including  $\Lambda$  spin-orbit splitting. This is most strikingly brought out in Fig. 11 for the 1850-Å film (the shift of the  $\Lambda$  peaks are discussed below). Even the 135-Å film, which is only about 25 atoms thick, reveals the structure predicted by bulk measurements, and, in fact, the proper structure was observed in still thinner films. Because of the agglomerate character of the films, this indicates that short-range order is far more important than long-range order in the formation of critical points in the band structure.

The RED patterns indicate the presence of stacking-fault and twin types of defects in each of our epitaxial films; however, what their effect should be in producing fine structure in the film optical response is not presently known.

The reflectivity amplitude of the 1850-Å film of Fig. 11 should in principle be equal to that of bulk germanium as its thickness is sufficient to suppress interference below 6000 Å. The reason it does not is due primarily to scattering from a rough surface arising from the agglomerate growth of the film. It has been shown by Porteus and Bennett<sup>28</sup> that the following relation for the reflectance of a rough surface,

$$R = R_0 \exp[-(4\pi\sigma/\lambda)^2], \quad (1)$$

where  $R_0$  is the reflectivity of a perfectly smooth surface of the same material and  $\sigma$  is the rms value of the deviations from mean thickness, is valid under the following assumptions:

(a) The surface irregularity distribution must be Gaussian.

(b) The reflected light must be coherently scattered from the surface, a condition which holds for  $\sigma/\lambda \ll 1$ . The ratio  $R(\text{film})/R(\text{bulk})$  for the 1850-Å film vs  $1/\lambda^2$  is given in Fig. 16. It is seen to yield approximately a straight line, in agreement with (1), whose slope determines a  $\sigma$  of 76 Å. By way of comparison, we might point out that the rms roughness of the usual variety of microscope slide is about 10–15 Å. Equation (1) predicts that as  $\lambda \rightarrow \infty$ ,  $R \rightarrow R_0$ ; however, Fig. 16 shows that  $R \rightarrow 0.091 R_0$ . This 9% difference can be explained as a constant systematic error in the film reflectivity due to misalignment and poor optical imaging because of the cleaved surface. For the 250-Å film of Figs. 12 and 13 we may perform a similar analysis by using only the reflectivity in the region below 3500 Å and extrapolating to infinite wavelength. In this region the skin depth is small (see Fig. 4) and interference does not occur. This procedure leads to  $\sigma = 50$  Å and  $R_\infty = 0.95 R_0$ . In addition, we see from Fig. 13 that roughness is not without its effect on the uv transmittance where  $T$  of the film falls below its theoretically predicted value by about 50% at  $\lambda = 2000$  Å.

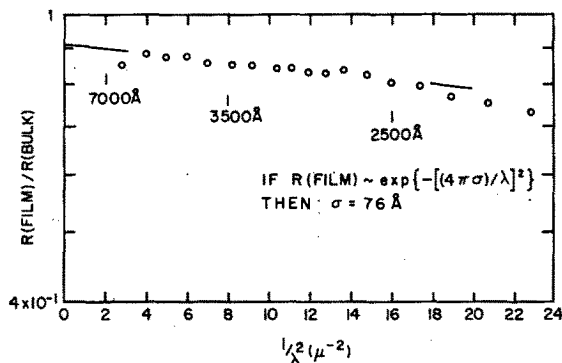


FIG. 16. Plot of  $R(\text{film})/R(\text{bulk})$  vs  $1/\lambda^2$  for the 1850-Å epitaxial Ge film on  $\text{CaF}_2$ .

<sup>28</sup> H. Bennett, J. Opt. Soc. Am. 53, 1389 (1963); J. Porteus, *ibid.* 53, 1394 (1963); H. Bennett and J. Porteus, *ibid.* 51, 123 (1961).

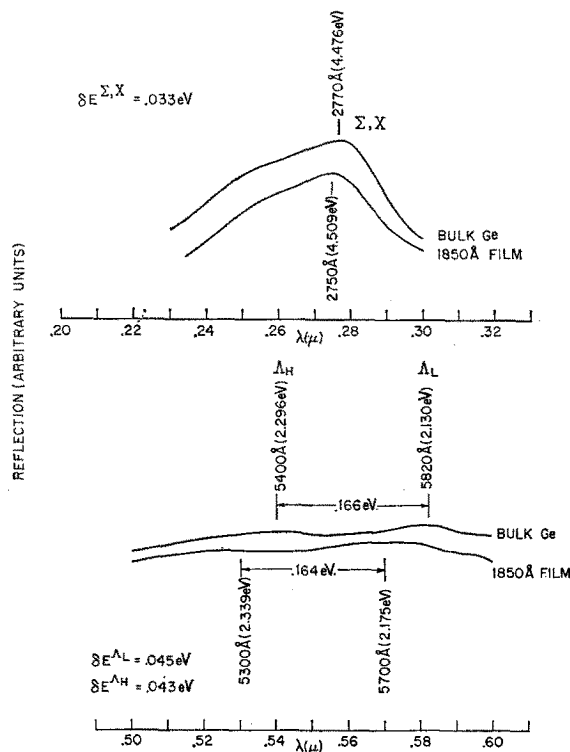


FIG. 17. Effect of film stress on the reflectivity peaks of the 1850-Å epitaxial Ge film on  $\text{CaF}_2$ .

Figures 14 and 15 show the optical response of a film whose thickness was measured by infrared transmission to be 135 Å. We see that the experimental values of  $R$  and  $T$  depart considerably from corresponding theoretical values,  $T$  measured being higher than  $T$  calculated (except in the far uv region) with the reverse true for  $R$ . The theoretical  $T$  and  $R$  are computed for a given film thickness using the data of Ref. 9 and the equations of Ref. 15. This behavior was observed in each of our very thin films; thus the film of Figs. 14 and 15 is not a mere variant. The disparity in amplitudes is probably due to the breakdown of coherent interference effects when the rms roughness of the film approaches an appreciable fraction of the mean film thickness. This results in phase averaging or intensity addition for the theoretical  $R$  and  $T$  expressions of Refs. 15 and 29. The effects of such averaging have been calculated and the results confirm the observed behavior. The scattering will not be nearly as strong for ir radiation; hence, measurements of transmission here can still be used to calculate thicknesses.

Surface roughness in epitaxial germanium films on  $\text{CaF}_2$  has been studied by Sloope and Tiller.<sup>23</sup> Their investigations indicate that conditions for good epitaxy are also conditions for appreciable roughness, and that the size of the agglomerates is of the order of some thousands of angstroms with thickness variations as much as 200 Å. Surface roughness is the most serious

<sup>23</sup> L. Harris, J. K. Beasley, and A. L. Loeb, J. Opt. Soc. Am. 41, 604 (1951). This paper contains a discussion of the appropriate phase-averaging procedures for thin-film formulas.



problem preventing the fabrication of films with bulk optical properties.

### C. Effect of Induced Strains in the Films on Optical Properties

Because of the difference in thermal expansion between film and substrate, there will appear an induced strain in the film as it is cooled from its formation temperature. The effect of this strain is clear from Fig. 17, where it is seen that both the  $\Lambda$  peaks and the  $\Sigma$ ,  $X$  peak are shifted to higher energies. In the discussion to follow, we make the following idealizations:

(a) The film and substrate are assumed to be isotropic, homogeneous, and temperature-independent in their thermal expansion properties.

(b) The film is assumed not to constrain the expansion of the substrate.

(c) The induced stress is considered as if it arose from forces applied at the faces of the film edges.

The constraining condition that gives us a relation for induced stress is that elongations of both film and substrate are necessarily equal. This leads to

$$X = (\alpha_{Ge} - \alpha_{CaF_2}) \Delta T / S, \quad (2)$$

where the  $\alpha$ 's are the appropriate linear thermal expansion coefficients,  $\Delta T$  the temperature change, and  $S$  and  $X$  are the appropriate inverse Young's modulus and induced stress, respectively, for the direction of elongation under consideration. For a film whose axis of epitaxy is  $[111]$ , the  $[1\bar{1}0]$  and  $[\bar{1}\bar{1}2]$  directions along with  $[111]$  form a mutually orthogonal set of which  $[1\bar{1}0]$  and  $[\bar{1}\bar{1}2]$  may be considered the directions of applied stress. For each of these directions,  $S$  becomes

$$S = \frac{1}{2}(s_{11} + s_{12} + s_{44}/2), \quad (3)$$

where  $s_{11}$ ,  $s_{12}$ , and  $s_{44}$  are the the compliance constants. For room-temperature values of  $\alpha_{Ge} = 5.75 \times 10^{-6}/^\circ\text{C}^{30}$  and  $\alpha_{CaF_2} = 19.5 \times 10^{-6}/^\circ\text{C}$ ,<sup>31</sup>  $s_{11} = 0.97 \times 10^{-6}/\text{atm}$ ,  $s_{12} = -2.63 \times 10^{-7}/\text{atm}$ , and  $s_{44} = 1.50 \times 10^{-6}/\text{atm}$ ,<sup>30</sup> with  $\Delta T = -575^\circ\text{C}$ , (2) and (3) give  $X = 10\,800$  atm compressive.

Brooks' equation for the shift of an energy band under strain may be written as<sup>32</sup>

$$\delta E = E_1 \text{Tr } \mathbf{u} + E_2 \hat{k} \cdot (\mathbf{u} - \frac{1}{3} \mathbf{1} \text{Tr } \mathbf{u}) \cdot \hat{k}. \quad (4)$$

Here  $E_1$  and  $E_2$  are deformation potentials,  $\hat{k}$  is the unit vector in  $\mathbf{k}$  space to the band edge in question, and  $\mathbf{u}$  is the strain tensor. We will take  $\delta E$ ,  $E_1$ , and  $E_2$  to refer to transitional energy differences instead of band edges. We note that in the case of hydrostatic pressure, Eq. (4) in conjunction with the generalized Hooke's law gives

$$\delta E = -3E_1(s_{11} + 2s_{12})X, \quad (5)$$

<sup>30</sup> *Selected Constants Relative to Semiconductors*, P. Aigrain and M. Balkanski, Eds. (Pergamon Press, Inc., New York, 1961).

<sup>31</sup> *Handbook of Chemistry and Physics* (Chemical Rubber Publishing Company, Cleveland, Ohio, 1955).

<sup>32</sup> H. Brooks, in *Advances in Electronics and Electron Physics*, L. Lorton, Ed. (Academic Press Inc., New York, 1956), Vol. 7; R. W. Keyes, in *Solid State Physics*, F. Seitz and D. Turnbull, Eds. (Academic Press Inc., New York, 1960), Vol. 11.

where  $X$  is the pressure. This relates  $E_1$  to the hydrostatic pressure coefficient  $\partial E/\partial P$ .

For applied biaxial stress  $X$  in the  $[1\bar{1}0]$  and  $[\bar{1}\bar{1}2]$  directions, the stress tensor is

$$\sigma = \frac{X}{3} \begin{pmatrix} 2 & -1 & -1 \\ -1 & 2 & -1 \\ -1 & -1 & 2 \end{pmatrix}. \quad (6)$$

Hooke's law and (4) yield for the ( $\Lambda_3 \rightarrow \Lambda_1$ ) transition in the  $[111]$  direction

$$\delta E_{[111]}^\Lambda = 2E_1^\Lambda(s_{11} + 2s_{12})X - \frac{1}{3}E_2^\Lambda s_{44}X. \quad (7)$$

On the other hand, for  $\Lambda$  transitions in  $[1\bar{1}1]$ -type directions, we have

$$\delta E_{[1\bar{1}1]}^\Lambda = 2E_1^\Lambda(s_{11} + 2s_{12})X + \frac{1}{3}E_2^\Lambda s_{44}X. \quad (8)$$

A similar analysis for the  $\Sigma$ ,  $X$  transition gives

$$\delta E_{[100]}^X = 2E_1^X(s_{11} + 2s_{12})X, \quad (9)$$

$$\delta E_{[110]}^\Sigma = 2E_1^\Sigma(s_{11} + 2s_{12})X - \frac{1}{6}E_2^\Sigma s_{34}X, \quad (10)$$

and

$$\delta E_{[1\bar{1}0]}^\Sigma = 2E_1^\Sigma(s_{11} + 2s_{12})X + \frac{1}{6}E_2^\Sigma s_{44}X. \quad (11)$$

We see that there is always a part related to hydrostatic pressure in addition to the shear component which lifts the degeneracy of otherwise equivalent transitions. The detection of this splitting was beyond the resolution of our experiments and its principal effect was probably to broaden slightly the reflectance peaks of the films.

Philipp, Dash, and Ehrenreich<sup>33</sup> have performed uniaxial stress measurements on the  $\Lambda$  transition of Ge. Using their value of  $E_2^\Lambda = -2.0$  eV<sup>34</sup> and  $E_1^\Lambda = -5.6$  eV calculated from Zallen's<sup>25</sup> value of the hydrostatic pressure coefficient, we obtain  $\delta E_{[111]}^\Lambda = (-4.0 \times 10^{-6} \text{ eV/atm})X$  and  $\delta E_{[1\bar{1}1]}^\Lambda = (-5.3 \times 10^{-6} \text{ eV/atm})X$ . As there are three times as many  $(1\bar{1}1)$  transitions as  $(111)$ , we take the over-all shift to be the weighted average of  $\delta E_{[111]}^\Lambda$  and  $\delta E_{[1\bar{1}1]}^\Lambda$  or  $\delta E^\Lambda = (-5.0 \times 10^{-6} \text{ eV/atm})X$ . From Fig. 17, we have  $\delta E^\Lambda = 44 \pm 10$  meV as the observed mean shift of the  $\Lambda$  doublet which implies a value of  $8800 \pm 2000$  atm for the induced biaxial compressive stress to be compared with 10 800 atm calculated from thermal expansion.

$E_1$  and  $E_2$  for the  $\Sigma$ ,  $X$  transition are not known at present. However, an estimate can be made of  $E_1$  from the pressure coefficient for the  $\Sigma$ ,  $X$  transition in silicon found by Zallen<sup>25</sup> to be about  $3 \times 10^{-6} \text{ eV/atm}$ . There is an empirical law which states that among semiconductors with similar band structures, the pressure coefficients for transitions between similar irreducible representations at identical points of their Brillouin zones are approximately equal.<sup>25,35</sup> We therefore take Zallen's result to hold for germanium also. For purposes of calculation, we will assume  $E_1^X = E_1^\Sigma$  and  $E_2^\Sigma = 0$ . From

<sup>33</sup> H. Philipp, W. Dash, and E. Ehrenreich, *Phys. Rev.* **127**, 762 (1962).

<sup>34</sup> This number was calculated from data contained in Refs. 33 and 25. The value of  $E_2$  actually given in Ref. 33 is believed to be in error.

<sup>35</sup> W. Paul, *J. Appl. Phys.* **32**, 2082 (1961).

Fig. 15,  $\delta E^{X,Z} = 33 \pm 12$  meV which results in  $X = 16\,500 \pm 6000$  atm compressive biaxial stress. The factor of two difference in the  $\Lambda$  and  $\Sigma$ ,  $X$  results cannot, at present, be attributed to anything except experimental error. Although a shift of reflectivity peaks was observed in all epitaxial films, it was carefully measured only in the 1850 Å film. Rather dramatic evidence of the film stress occurs as the film is made thicker. Since the stress force is applied at the film-substrate interface, a bending moment is created in the film which increases with film thickness until some critical value is reached whereupon the film begins to break away from the substrate. For a substrate temperature of 600°C, the critical thickness appears to be around 3000–4000 Å as deduced from observations of thick films that rapidly broke up immediately after deposition.

#### IV. CALCULATION OF THE FILM OPTICAL CONSTANTS

The theory necessary for the deduction of the optical constants from measurements of thin-film reflectivity and transmissivity is discussed elsewhere<sup>15</sup> and only the principal conclusions and results are presented here. Using appropriate theoretical expressions for  $R$  and  $T$ , the optical constants may be recovered through a Newton-Raphson iteration using a high-speed digital computer. In doing this, it is found that there are certain regions in which the derived  $n$  and  $k$  are very sensitive to small changes in  $R$  and  $T$ . This fact, however, is shown in Ref. 15 to be intrinsic in the theoretical development and is not connected with any particular method of numerical analysis. The sensitivity to experimental error arises from the existence of at least one branch point in the dependence of  $n$  and  $k$  on  $R$  and  $T$ . The branch point originates from the fact that

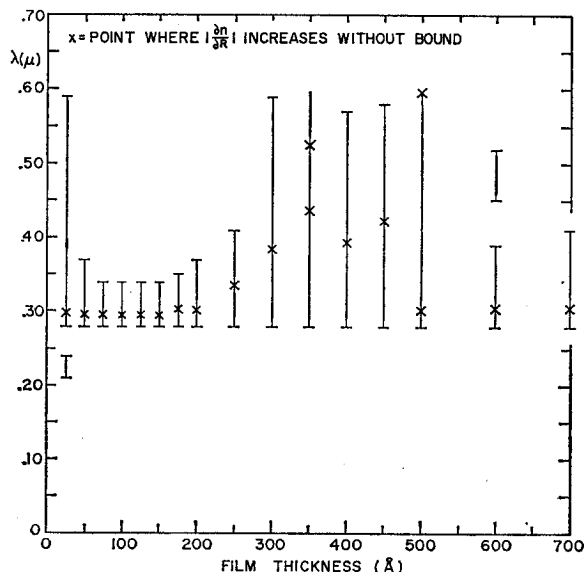


FIG. 18. Wavelength region where  $|\partial n/\partial R| \geq 20$  as a function of film thickness. The optical constants of Ge from Ref. 9 were used in Ref. 15 to calculate this bar diagram. The criterion on  $|\partial n/\partial R|$  was determined by stipulating that an error of 0.5 absolute in the derived  $n$  would be considered intolerable for an error of 2.5% absolute in the measured  $R$ .

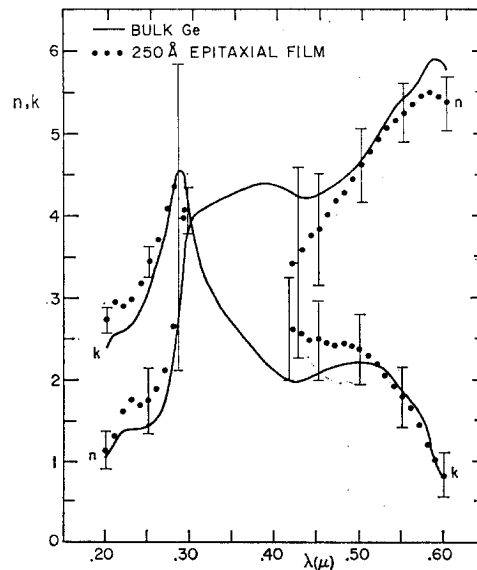


FIG. 19. Optical constants derived from  $R$  and  $T$  measurements on a 250-Å epitaxial germanium film deposited on  $\text{CaF}_2$ .

$R$  and  $T$  are intensities and involve squares of the optical constants. It turns out that the most critical behavior is that of the real part of the index of refraction on reflectivity. Figure 18 indicates that there is always some wavelength region for which  $n$  is highly sensitive to small experimental errors in  $R$ . In fact, there is always at least one singular point in  $|\partial n/\partial R|$ . However, there appears to be an optimum film thickness range, although experimental considerations may obviate its use. In our work, we found 250 Å to be a workable thickness in both experimental and theoretical aspects and we present the results for this film in Fig. 19. In performing the calculation, the reflectivity in Fig. 12 was corrected for roughness scattering according to the experimental quantities  $R_\infty = 0.95R_0$  and  $\sigma = 50$  Å. These quantities were calculated by extrapolating from the high absorption region and applying Eq. (1). The bars indicate the error spread in  $n$  and  $k$  for an absolute error in  $R$  of  $\pm 2.5\%$  and in  $a$  of  $\pm 10$  Å, and a relative error in  $T$  of  $\pm 10\%$ . We see that the discrepancy between the film values of the optical constants and those of bulk Ge (taken from Fig. 3) can be included, for the most part, within the span of these conservative experimental estimates. We see also that in the region in which no roots appeared, namely, 3000 to 4100 Å, corresponds almost exactly to the region predicted by Fig. 18 for a 250-Å film as having very high sensitivity to experimental errors in  $R$  and  $T$ . Reference to Figs. 5 and 6 shows that the present results are far superior to previous film optical constant work, primarily because of the use of epitaxial films.

#### V. CONCLUSIONS

In Sec. I it was stated that the object of this research was to study the correlation between the optical properties of semiconductors in the film and bulk states using germanium as the investigative medium. We believe the following to be the three main conclusions:

(a) A correspondence can be established between the crystalline perfection of a film as determined by diffraction techniques and the degree to which its optical spectrum approaches that of a bulk single crystal. It is interesting to note that although the grain size of our very thin epitaxial films approximated that of the polycrystalline films, only the former possessed bulk optical structure. This would suggest that it is some other factor, such as large intrinsic strain, rather than small grain size that distorts the optical response of our polycrystalline films. However, the exact nature of the relation between grain size, texturization, intrinsic strain, etc., and the band structure of a disordered material is a subject which remains for future theoretical and experimental development.

(b) We feel our measurements of  $R$  and  $T$  and calculations of  $n$  and  $k$  indicate that after experimental difficulties have been taken into account the epitaxial films have essentially the same optical properties as bulk material. Hence we may consider the use of epitaxial films as reliable vehicles for investigation into the optical properties of semiconductors in the high-absorption regions.

(c) However, because the theoretical discussions of Sec. IV indicate that there will invariably be a region of high sensitivity in the derived  $n$  and  $k$  to errors in  $R$  and  $T$ , we may conclude that film determinations of  $n$  and  $k$  will not supplant, but rather will supplement, other methods such as polarimetry and dispersion analyses. We have shown that in the regions where roots are obtained, the film optical constants compare favorably with the Kramers-Kronig result.

With regard to the statement in (b) concerning experimental difficulties, we believe these to be of four types:

(1) *Roughness scattering.* As pointed out in Sec. III, the deposition conditions for epitaxial films are in opposition to the requirements for smooth films and this prevents attainment of bulk single-crystal optical properties. However, there is evidence that the situation is not so severe in the case of epitaxial lead salt films.<sup>36</sup> Extensions of this work should concentrate on devising methods of producing smooth films, possibly through techniques other than vacuum deposition.

(2) *Cleaved surfaces.* The result was to produce systematic errors in the reflectivity and transmissivity amplitudes (less so in the latter than in the former). Careful selection of the sample area to be studied helped minimize this difficulty.

(3) *Reflectometer misalignment.* Because the reflected ray does not follow the same optical path as the incident ray, there is always some difficulty in aligning to measure absolute reflectivity. In our work, we used as an alignment standard a very carefully etched sample of bulk germanium. In this way we were able to reduce errors by periodically checking our film alignment procedures with our standard.

<sup>36</sup> P. R. Wessel (to be published); C. E. Rossi, Gordon McKay Laboratory of Applied Science, Harvard University (unpublished data.)

(4) *Stress effects.* In Sec. III, the energy shift in the characteristic film reflectivity peaks due to the difference in the thermal expansion coefficients of the film and substrate was discussed. As a result, we must be cautious in ascribing structure appearing in film optical spectra as being precisely at the same energy as it would appear in the bulk material. Particular care is to be exercised in assigning physical significance to energy differences between absorption edges in films and reflectivity peaks in bulk crystals. On the other hand, in relation to the entire film optical response spectrum considered here (2–6 eV) the effect is small ( $\sim 40$  meV) and may usually be ignored.

Because of the roughness-coherence difficulties, we were not able to investigate the effect of thickness on the film optical properties. The influence of this parameter seems to be divided into two aspects: (1) the perturbative effect of the finite boundary on the bulk energy levels, and (2) the "quantization" of  $k$  space in the direction normal to the film surface into intervals of  $2\pi/Na$ , where  $N$  is the number of atoms and  $a$  the lattice constant. Of these, the second has the interesting possibility of giving the density of states a two-dimensional character and of splitting interband transitions which occur between bands of nonzero slope. Such splittings may be hard to observe, however, due to competition from other directions in the Brillouin zone equivalent to the thickness direction.

It is possible to conceive of several experiments in the range 2–6 eV for which epitaxial films would be particularly suitable; for example, magneto-optic measurements such as magnetoabsorption and Faraday and Voigt effects, hydrostatic pressure shifts, and photoconductivity investigations are some that can be considered. In addition, it may prove more feasible to produce certain semiconductor alloys in film form than in the bulk state in order to study their optical properties.

## ACKNOWLEDGMENTS

The authors wish to thank Dr. H. R. Philipp, T. M. Donovan, and P. Wessel for providing them with preprints of their work prior to publication and to acknowledge a useful correspondence with B. W. Sloope on the preparation and properties of epitaxial germanium films. Thanks are also due to Dr. G. Via and Dr. M. Holland for the use of their vacuum apparatuses during certain stages of this work.

The authors have also benefited from discussions with colleagues of the Gordon McKay Laboratory and wish to thank B. Kosicki, P. McElroy, and R. Ludeke for suggestions concerning the experimental apparatus and C. Rossi and Dr. R. Zallen for discussion of the experimental results.

The construction of all experimental apparatuses was performed by James Inglis and Albert Manning while David MacLeod assisted in sample preparation.

One of us (PMG) wishes to acknowledge the personal financial assistance provided by the IBM Corporation over the duration of this research.